 doi:10.20944/preprints202104.0249.v1

Effect of Thermal Radiation on the Conjugate Heat Transfer from a Circular Cylinder with an Internal Heat Source in Laminar Flow

Gheorghe Juncu

POLITEHNICA University Bucharest

Department of Chemical and Biochemical Engineering

Polizu 1, 011061 Bucharest

Romania

Phone: + 40 21 312 6879

Fax: + 40 21 312 6879

E-mail: juncu.gheorghe@yahoo.com

juncu@cael.pub.ro

 doi:10.20944/preprints202104.0249.v1

Abstract

The effect of thermal radiation on the two – dimensional, steady-state, conjugate heat transfer from a circular cylinder with an internal heat source in steady laminar crossflow is investigated in this work. P_0 (Rosseland) and P_1 approximations were used to model the radiative transfer. The mathematical model equations were solved numerically. Qualitatively, P_0 and P_1 approximations show the same effect of thermal radiation on conjugate heat transfer; the increase in the radiation – conduction parameter decreases the cylinder surface temperature and increases the heat transfer rate. Quantitatively, there are significant differences between the results provided by the two approximations.

Keywords: conjugate heat transfer; convection-radiation; Rosseland approximation; P_1 approximation; finite difference; defect correction - multigrid.

Preprints (www.preprints.org) | NOT PEER-REVIEWED | Posted: 8 April 2021 doi:10.20944/preprints202104.0249.v1

NOMENCLATURE

a	radius of the cylinder, m
$\mathfrak{B}$	dimensionless group, $\mathfrak{B}= 3\,\beta\,a$
c_P	heat capacity, J / (kg K)
d	diameter of the cylinder, $d = 2\,a$, m
$\mathcal{E}$	dimensionless group, $\mathcal{E} = \frac{\varepsilon}{2\,(2-\varepsilon)}$
G	dimensionless directed – integrated intensity of the radiation, $G = \frac{G^*}{4\,n^2\,\sigma\,T_0^4}$
G^*	dimensional directed – integrated intensity of the radiation, W / m^2
k_a	absorption coefficient, m^{-1}
$\mathcal{K}$	dimensionless group, $\mathcal{K}= k_a\,a$
n	index of refraction, dimensionless
Nu	average Nusselt number, dimensionless
$Nu\,(\theta)$	local Nusselt number, dimensionless
Pr	Prandtl number, $Pr = \mu_f\ / \rho_f\,\alpha_f$, dimensionless
q_r	dimensionless radiative heat flux vector
Re	cylinder Reynolds number, $Re = U_\infty\,d\ \rho_f\ / \mu_f$, dimensionless
Rd_0	Rosseland radiation - conduction parameter, dimensionless
Rd_1	radiation - conduction parameter for P_1 approximation, dimensionless
r	dimensionless radial coordinate, r^* / a, in cylindrical coordinate system
r^*	radial coordinate in cylindrical coordinate system, m
r_0	dimensionless radius of the wire

Preprints (www.preprints.org) | NOT PEER-REVIEWED | Posted: 8 April 2021 doi:10.20944/preprints202104.0249.v1

T temperature, K

U_∞ velocity far away from the cylinder, m / s

V_R dimensionless radial velocity component

V_θ dimensionless tangential velocity component

Z dimensionless temperature defined by the relation, $Z_{f(c)} = \frac{T_{f(c)} - T_\infty}{T_0 - T_\infty}$

Greek symbols

α thermal diffusivity, m^2 / s

β extinction coefficient (total attenuation factor), m^{-1}

β_R Rosseland mean extinction coefficient, m^{-1}

ε emissivity coefficient, dimensionless

ζ temperature ratio, $\zeta = \frac{T_\infty}{T_0}$, dimensionless

Φ thermal conductivity ratio, λ_c / λ_f, dimensionless

λ thermal conductivity, W / (m K)

μ dynamic viscosity, kg / (m s)

θ polar angle in cylindrical coordinate system, rad

ρ density, kg / m^3

σ Stefan – Boltzman constant, $\sigma = 5.670 \times 10^{-8}$ W (m^2 K^4)

 doi:10.20944/preprints202104.0249.v1

Subscripts

c	refers to the physical property of the cylinder
f	refers to physical property of the fluid
inf	refers to a large finite distance from the center of the cylinder
s	refers to the surface of the cylinder
0	refers to the wire inserted into the cylinder

 doi:10.20944/preprints202104.0249.v1

1. Introduction

All materials with the temperature in the range of 30 to 30,000 K emit and absorb thermal radiation. The emission of thermal radiation is due to the conversion of the internal energy into energy transported by electromagnetic waves or photons. For heat transfer applications wavelengths between 10^{-7} m and 10^{-3} m are important.

The radiative transfer equation (RTE) is an integro–differential equation very difficult to solve. Exact analytical solutions exist only for simple situations such as one – dimensional plane parallel media without scattering. Therefore, approximate mathematically less complicated but accurate models for the RTE have been developed. Examples are zeroth order diffusion or Rosseland approximation [1], high order diffusion approximations like P_N [2] and SP_N [3], and the moments method [4], [5] (and the references quoted herein). The numerical methods proven to be effective for solving RTE are the zonal method [1], the discrete ordinates method [6] (and the references quoted herein), the finite volume method [6] (and the references quoted herein) and the finite element method [7, 8]. The Monte Carlo [9] and the lattice Boltzmann [10] methods were also used to solve RTE. An extensive presentation of these approximate models is outside the aims of the present work. Reviews can be viewed in [1] and [11].

The RTE solving necessitates the knowledge of the temperature profiles. In almost all the articles that investigate the RTE solving, the energy balance equation considered is the one phase, transient heat conduction equation. The influence of thermal radiation on more complex heat transfer problems was investigated by (the citation is restricted to the cases of forced / mixed convection – radiation heat transfer in external flows) Hossain and Takhar [12], Andrienko et al. [13], Zhang et al. [14], Surzhikov [15], Sheikholeslami and Shehzad [16], Waqas et al. [17], Imtiaz et al. [18], Irfan et al. [19], Roy and Gorla [20]. The boundary layer formalism and Rosseland approximation were used in [12], [14], [17 – 20]. Sheikholeslami and Shehzad [16] solved numerically the 2D mass, momentum and energy balance equations using the Rosseland approximation to model the radiative heat transfer. Complex models for mass, momentum, energy and chemical species conservation equations coupled with RTE were solved numerically by Andrienko et al. [13] and Surzhikov [15] in 2D axisymmetric and 3D geometries.

Preprints (www.preprints.org) | NOT PEER-REVIEWED | Posted: 8 April 2021 doi:10.20944/preprints202104.0249.v1

The effect of thermal radiation on conjugate, forced convection heat transfer was analysed only for an internal flow problem by Nia and Nassab [21, 22]. The aim of the present work is to investigate the effect of thermal radiation on the conjugate, forced convection heat transfer for the external flow case. To the best of our knowledge, this problem is reported for the first time here. The test problem models the steady – state conjugate heat transfer from a circular cylinder with an internal heat source in steady laminar crossflow. The P_0 (Rosseland) and P_1 approximations were used to model the radiative transfer.

This paper is organized as follows. In Sect. 2 we describe the mathematical model of the problem. Section 3 presents the numerical algorithm. The numerical experiments made and the results obtained are presented in Sect. 4. Finally, some concluding remarks are briefly mentioned in Sect. 5.

2. Mathematical model

Let us consider an infinitely long horizontal circular cylinder placed in a vertical, laminar, steady flow of an incompressible Newtonian fluid (see figure 1). The diameter of the cylinder d is assumed considerably higher than the mean free path of the surrounding fluid. Inside the cylinder there is a wire of dimensionless radius r_0 and constant temperature T_0. The free stream velocity and temperature of the fluid are U_∞ and T_∞, respectively ($T_0 > T_\infty$). The physical properties of the cylinder and surrounding fluid are constant and isotropic. The effects of buoyancy, viscous dissipation and work done by pressure forces are considered negligible. The fluid is assumed to be a gray, emitting, absorbing and isotropic scattering medium.

For the assumptions discussed previously, the dimensionless energy balance equations (the radius of the cylinder a is considered the length scale and the free stream velocity U_∞ the velocity scale), expressed in dimensionless cylindrical coordinate system (r, θ), are:

- Inside the cylinder;

($r \leq r_0$),

$$Z_c = 1.0; \tag{1a}$$

Preprints (www.preprints.org) | NOT PEER-REVIEWED | Posted: 8 April 2021 doi:10.20944/preprints202104.0249.v1

($r_0 < r < 1$),

$$\frac{1}{r}\frac{\partial}{\partial r}\left(r\,\frac{\partial Z_c}{\partial r}\right)+\frac{1}{r^2}\frac{\partial^2 Z_c}{\partial \theta^2}=0 \tag{1b}$$

- In the surrounding fluid;

$$\frac{Re\,Pr}{2}\left(V_R\,\frac{\partial Z_f}{\partial r}+\frac{V_\theta}{r}\frac{\partial Z_f}{\partial \theta}\right)=\frac{1}{r}\frac{\partial}{\partial r}\left(r\,\frac{\partial Z_f}{\partial r}-r\,q_{r,r}\right)+\frac{1}{r^2}\frac{\partial}{\partial \theta}\left(\frac{\partial Z_f}{\partial \theta}-q_{r,\theta}\right) \tag{2}$$

where $q_{r,r}$ and $q_{r,\theta}$ are the dimensionless normal and tangential components of the radiative heat flux vector.

The boundary conditions to be satisfied by the dimensionless temperature are:

- Symmetry axis ($\theta = 0, \pi$);

$$\frac{\partial Z_c}{\partial \theta}=0,\frac{\partial Z_f}{\partial \theta}=0 \tag{3a}$$

- Interface ($r = 1$);

$$\Phi\frac{\partial Z_c}{\partial r}=\frac{\partial Z_f}{\partial r}-q_r \tag{3b}$$

- Free stream ($r \to \infty$);

$$Z_f = 0.0 \tag{3c}$$

Rosseland approximation

The radial and tangential components of the dimensionless radiative heat flux vector given by Rosseland approximation [1] read as:

$$q_{r,r}=-\frac{4}{3}\,Rd_0\left[\zeta+Z_f\,(1-\zeta)\right]^3\frac{\partial Z_f}{\partial r},q_{r,\theta}=-\frac{4}{3}\,Rd_0\left[\zeta+Z_f\,(1-\zeta)\right]^3\frac{\partial Z_f}{\partial \theta}. \tag{4}$$

where Rd_0 is the Rosseland radiation – conduction parameter, $Rd_0 = 4\,\sigma\,T_0^3/(\lambda_f\,\beta_R)$ and $\zeta = \frac{T_\infty}{T_0}$. Note that

$$\zeta+Z_f\,(1-\zeta)=\frac{T}{T_0}$$

Preprints (www.preprints.org) | NOT PEER-REVIEWED | Posted: 8 April 2021 doi:10.20944/preprints202104.0249.v1

If we denote, for the simplicity of writing, $f = \frac{4}{3}\, Rd_0 \left[\, \zeta + Z_f \,(1 - \zeta)\,\right]^3$, equation (2) can be rewritten as

$$\frac{Re\, Pr}{2}\left(V_R\, \frac{\partial Z_f}{\partial r} + \frac{V_\theta}{r}\, \frac{\partial Z_f}{\partial \theta}\right) = \frac{1}{r}\, \frac{\partial}{\partial r}\left[r\,(1+f)\, \frac{\partial Z_f}{\partial r}\right] + \frac{1}{r^2}\, \frac{\partial}{\partial \theta}\left[(1+f)\, \frac{\partial Z_f}{\partial \theta}\right] \tag{5}$$

P_1 approximation

For P_1 approximation, the dimensionless radiative heat flux vector satisfies the equation, [1],

$$\frac{1}{r}\, \frac{\partial}{\partial r}\left(r\, q_{r,r}\right) + \frac{1}{r^2}\, \frac{\partial\, q_{r,\theta}}{\partial\, \theta} = -\,\mathcal{K}^2\, \frac{Rd_1}{1-\zeta}\left\{\left[\zeta + Z_f\,(1-\zeta)\right]^4 - G\right\} \tag{6}$$

where G is the dimensionless directed – integrated intensity of the radiation, $\mathcal{K} = k_a\, a$, $Rd_1 = 4\,\sigma\, n^2\, T_0^3 \,/\left(k_a\, \lambda_f\right)$. Substituting equation (6) into equation (2), it results:

$$\frac{Re\, Pr}{2}\left(V_R\, \frac{\partial Z_f}{\partial r} + \frac{V_\theta}{r}\, \frac{\partial Z_f}{\partial \theta}\right) = \frac{1}{r}\, \frac{\partial}{\partial r}\left(r\, \frac{\partial Z_f}{\partial r}\right) + \frac{1}{r^2}\, \frac{\partial^2 Z_f}{\partial \theta^2} - \mathcal{K}^2\, \frac{Rd_1}{1-\zeta}\left\{\left[\zeta + Z_f\,(1-\zeta)\right]^4 - G\right\} \tag{7}$$

Note that some elementary algebraic manipulations were made in order to obtain for Rd_1 an expression similar to that for Rd_0. The dimensionless directed – integrated intensity of radiation G verifies the equation [1]:

$$\frac{1}{r}\, \frac{\partial}{\partial r}\left(r\, \frac{\partial G}{\partial r}\right) + \frac{1}{r^2}\, \frac{\partial^2 G}{\partial \theta^2} - \mathfrak{B}\,\mathcal{K}\left\{G - \left[\zeta + Z_f\,(1-\zeta)\right]^4\right\} = 0 \tag{8}$$

where $\mathfrak{B} = 3\,\beta\, a$.

The boundary conditions to be satisfied by G are, [1]:

- Symmetry axis ($\theta = 0, \pi$);

$$\frac{\partial G}{\partial \theta} = 0 \tag{9a}$$

- Interface ($r = 1$);

$$-\,\frac{\partial G}{\partial r} + \mathfrak{B}\,\mathcal{E}\left\{G - \left[\zeta + Z_f\,(1-\zeta)\right]^4\right\} = 0 \tag{9b}$$

Preprints (www.preprints.org) | NOT PEER-REVIEWED | Posted: 8 April 2021 doi:10.20944/preprints202104.0249.v1

- Free stream ($r \rightarrow \infty$);

$$\frac{\partial G}{\partial r} + \frac{1}{2} \mathfrak{B} G = 0 \tag{9c}$$

or

$$G = \zeta^4 \tag{9d}$$

where $\mathcal{E} = \frac{\varepsilon}{2(2-\varepsilon)}$. Two boundary conditions were proposed and tested for G at free stream. The boundary condition (9c) considers the free stream as an inflow / outflow boundary with null intensity of radiation. The boundary condition (9d) assumes radiative equilibrium at free stream.

It must be mentioned that for the P_1 approximation, the dimensionless radiative heat flux is given by [1],

$$q_r = -1 / \mathfrak{B} \textbf{ grad } G. \tag{10}$$

The physical quantities of interest are the cylinder surface dimensionless average temperature $\bar{Z}_{c,s}$, the local Nusselt number, Nu (θ), and the average Nusselt number, Nu. Considering as driving force the difference (T_0 - T_∞), the local Nusselt number based on the diameter of the cylinder is given by (for $\Phi \geq 1$):

$$Nu(\theta) = -2 \Phi \left.\frac{\partial Z_c}{\partial r}\right|_{r=1-} \tag{11}$$

The average Nu number is given by the relation:

$$Nu = \frac{1}{\pi} \int_0^\pi Nu(\theta)\, d\theta \tag{12}$$

The cylinder surface dimensionless average temperature $\bar{Z}_{c,s}$, was computed with the relations:

$$\bar{Z}_{c,s} = \frac{2}{\pi} \int_0^\pi Z_c|_{r=1}\, d\theta \tag{13}$$

Preprints (www.preprints.org) | NOT PEER-REVIEWED | Posted: 8 April 2021 doi:10.20944/preprints202104.0249.v1

3. Method of solution

The energy balance equations (1, 2) belong to the class called *interface problem*, [23]. The spatial derivatives (equations (1b, 2) were rewritten as a single equation with discontinuous coefficients) were discretized with the upwind and centered finite difference schemes (a double discretization required by the defect – correction iteration) on a vertex-centered grid, [23]. The spatial derivatives of the radiative transfer equation (8) were approximated by the centered finite difference scheme. Numerical experiments were made on meshes with the discretization steps, $\Delta\theta = \pi / 128$, $\Delta r = 1 / 128$, $\Delta\theta = \pi / 256$, $\Delta r = 1 / 256$, $\Delta\theta = \pi / 512$, $\Delta r = 1 / 512$ and $\Delta\theta = \pi / 1024$, $\Delta r = 1 / 1024$. The external boundary conditions (3c) and (9c, d) are assumed to be valid at a large but finite distance, $r_{inf,}$ from the center of the cylinder. The algorithm used to solve the discrete equations is the nested multigrid defect-correction iteration presented by Juncu and Mihail [24].

The defect – correction iteration was applied only to the discrete approximation of the energy balance equation. Two multigrid cycles were used inside the defect – correction iteration step. The structure of the multigrid cycle is: 1) cycle of type V; 2) smoothing by alternating line Gauss Seidel method; 3) two smoothing steps are performed before the coarse grid correction and one after; 4) prolongation by bilinear interpolation for corrections; 5) restriction of residuals by full weighting. The velocity field (V_R, V_θ) were calculated solving numerically the Navier-Stokes equations. More information about the hydrodynamic computations can be viewed in [24, 25].

The error criteria employed are: the discrete L_2 norm of the residuals and the discrete L_∞ norm of the difference between the numerical solutions of two consecutive defect - correction iterations are smaller than 10^{-8}. Results that can be used to validate the accuracy of the present heat transfer computations are not available in literature. The mesh independence of the *Nu* number and dimensionless cylinder surface temperature was the accuracy test used in the present computations.

Preprints (www.preprints.org) | NOT PEER-REVIEWED | Posted: 8 April 2021 doi:10.20944/preprints202104.0249.v1

4. Results and discussions

The dimensionless groups of the present problem can be divided into the following two classes: (1) conjugate convection – diffusion heat transfer dimensionless groups, Pr, Re, Φ and ζ; (2) radiative dimensionless groups, $\mathfrak{B}$, $\mathcal{E}$, $\mathcal{K}$ and $Rd_{0(1)}$.

The assumption of steady laminar flow imposes $Re \leq Re_{crt} \cong 46$. The numerical values considered for the Pr number are, $Pr \geq 1.0$. The thermal conductivity ratio, Φ, takes values from 1 to 10^2. For values of Φ little than 1.0, the values of the dimensionless cylinder surface temperature are very small (for example, for $\Phi = 0.1$, $\bar{Z}_{c,s} < 0.1$). In this case the effects of the radiative heat transfer become negligible. The values of the radiative dimensionless groups $\mathfrak{B}$, $\mathcal{E}$ and $\mathcal{K}$ are given by the values of a, k_a, β and ε. The numerical values considered for the radius of the cylinder are in the range, 0.01 m $\leq a \leq$ 10 m. The values of k_a and β were taken from [1]. The emissivity ε takes values in the range, $0.5 \leq \varepsilon \leq 0.9$. The values considered for the radiation – conduction parameters $Rd_{0(1)}$ are, $0 < Rd_{0(1)} \leq 1000$. In all computations ζ was considered equal to $\zeta = 0.833333$ ($T_0 / T_\infty = 1.2$).

The quantities used to quantify the influence of the thermal radiation on the conjugate heat transfer are the ratios:

$$\eta_s = \frac{\bar{Z}_{c,s}\,(Rd \neq 0)}{\bar{Z}_{c,s}\,(Rd = 0)};\ \ \eta_N = \frac{Nu\,(Rd \neq 0)}{Nu\,(Rd = 0)}.$$

In the next paragraphs, the ratios η_S and η_N will be called surface ratio and flux ratio, respectively. The effect of thermal radiation on the conjugate heat transfer is considered significant when

$$|\,\eta_N - 1\,| > 0.1.$$

The first aspect analysed is the influence of the boundary conditions (9c) and (9d) on the numerical solution of the P_1 model. Figure 2 shows that the numerical solution calculated with the boundary condition (9c) is very sensitive to the value of r_{inf}. When r_{inf} increases, the numerical solution calculated with the boundary condition (9c) tends to the numerical solution calculated with the boundary condition (9d). Otherwise, the influence of the values of r_{inf} on the numerical solution calculated with the boundary condition (9d) is negligible (obviously, the previous

Preprints (www.preprints.org) | NOT PEER-REVIEWED | Posted: 8 April 2021 doi:10.20944/preprints202104.0249.v1

statements are valid for values of r_{inf} usually used in the analysis of the heat transfer from circular cylinders in steady flows). For these reasons, the numerical solutions presented in the next paragraphs for the P_1 model were calculated with the boundary condition (9d).

The influence of the thermal radiation on the conjugate heat transfer is presented in figures 3 – 7. The numerical data plotted in figures 3 to 7 represents a selection from the numerical experiments made. This selection captures the salient features of the process. From the numerical results obtained the following remarks can be made:

- Qualitatively, the effect of the thermal radiation on the conjugate heat transfer is the same for both P_0 and P_1 models; the increase in the radiation – conduction parameter decreases the dimensionless surface temperature of the cylinder and increases the *Nu* number;
- Quantitively, in spite of the fact that a relation between Rd_0 and Rd_1 is difficult to find, there are significant differences between the results provided by the P_0 and P_1 models; the relation between Rd_0 and Rd_1 is given by the relation between k_a and β_R; according to Modest [1], the relations used to calculate the Rosseland mean extinction coefficient β_R are questionable; usually, one can assume $\beta_R > k_a$ but not $\beta_R >> k_a$;
- For the P_0 model, the effect of the thermal radiation on the conjugate heat transfer becomes significant when $Rd_0 > 0.1$;
- For the P_1 model, the effect of the thermal radiation on the conjugate heat transfer becomes significant when $Rd_1 > 100$ regardless the values of the other parameters; however, the effect of the other radiation parameters on the conjugate heat transfer can not be considered negligible; the increase in the absorption coefficient k_a increases the effect of thermal radiation on the conjugate heat transfer while the increase in the total attenuation factor β and the emissivity coefficient ε decreases the effect of thermal radiation on the conjugate heat transfer;
- Based on the numerical experiments made, one can state that for the P_1 model the effect of thermal radiation on the conjugate heat transfer becomes significant when,

$$\frac{\frac{\mathcal{K}^2\, Rd_1}{1-\zeta}}{\mathfrak{B}\,\mathcal{K}} = \frac{\mathcal{K}\, Rd_1}{\mathfrak{B}\,(1-\zeta)} > 100$$

Preprints (www.preprints.org) | NOT PEER-REVIEWED | Posted: 8 April 2021 doi:10.20944/preprints202104.0249.v1

- The increase in the conductivity ratio Φ decreases the values of the surface ratio η_S and increases the values of the flux ratio η_N;
- The increase in the convection rate (e.g. the product *Re Pr*) decreases the effect of thermal radiation;
- The increase in the wire dimensionless radius r_0 increases the cylinder surface dimensionless temperature and *Nu* number.

The P_0 approximation reduces the radiation – convection – conduction problem to a standard convection – conduction problem with strongly temperature dependent thermal conductivity. The increase in the thermal conductivity of the fluid decreases the temperature gradient at the interface but amplifies the heat flux. The global result is the enhancement of the heat transfer rate even for small values of Rd_0. It must be also mentioned that, for the Rosseland approximation, the same results were obtained neglecting the radiation transfer in the tangential direction.

In a first approximation, one can consider the P_1 model similar to the model of mass transfer accompanied by a reversible chemical reaction with an unusual reaction rate and equilibrium constant equal to unity (see for example [26]). The dimensionless temperature is the reactant of the reversible chemical reaction while the dimensionless directed – integrated intensity of the radiation is the product of the reversible chemical reaction. However, there are differences between the present mathematical model and the mathematical model for the mass transfer accompanied by a reversible chemical reaction. In the case of the mass transfer accompanied by a reversible chemical reaction all the species involved in process obey the same mass transfer mechanism, convection – diffusion – reaction. For the present mathematical model, equation (7) is a convection – diffusion – reaction equation while equation (8) is a diffusion – reaction equation. For any convection – diffusion – reaction equation a boundary layer with variable thickness develops on the surface of the cylinder from the region of the front stagnation point. The thickness of the boundary layer depends on the value of the product *Re Pr*. Outside the boundary layer the numerical values of the variables are approximately constant. For a diffusion – reaction problem the boundary layer does not occur. A diffusion film of constant thickness may occur in some conditions. The coupling and interaction between the solution of a convection – diffusion – reaction equation (the dimensionless temperature) and the solution of a diffusion – reaction equation (the dimensionless directed – integrated intensity of the radiation) explains the features of the present P_1 solution.

Preprints (www.preprints.org) | NOT PEER-REVIEWED | Posted: 8 April 2021 doi:10.20944/preprints202104.0249.v1

The effect of the order of approximation of spherical harmonics model on the solution of the present problem is the last issue discussed in this section. The results presented in [1] and [27] for a thick medium show that the differences between the P_1 approximation, high order spherical harmonics approximations and the solution of the full radiative transfer equation are small. Significant differences exist between the P_0 approximation, high order spherical harmonics approximations and the solution of the full radiative transfer equation. Thus, one can consider the P_1 approximation used in this work an efficient and sufficiently accurate solution for the present radiative heat transfer problem (the optical thickness for the present medium is very large).

5. Conclusions

The effect of thermal radiation on the steady-state, conjugate heat transfer from a circular cylinder with an internal heat source in steady laminar crossflow was analysed in this work. The radiative transfer is modeled by the P_0 (Rosseland) and P_1 approximations. Two free stream boundary conditions are tested for the dimensionless directed – integrated intensity of the radiation (P_1 approximation).

The effect of the thermal radiation on the conjugate heat transfer consists of the increase in the Nu number and the decrease in the cylinder surface temperature. As expected, for both approximations, the increase in the radiation – conduction group increases the effect of the thermal radiation on the conjugate heat transfer. However, there are significant quantitative differences between the results provided by the P_0 and P_1 approximations. For the P_1 approximation, the increase in the absorption coefficient k_a and the decrease in the total attenuation factor β and the emissivity coefficient ε increase the effect of thermal radiation on the conjugate heat transfer.

 doi:10.20944/preprints202104.0249.v1

References

[1] M.F. Modest, *Radiative Heat Transfer*, 3rd ed., pp. 483, 585 – 606, 502 – 509, 761, Academic Press, Oxford, 2013.

[2] M. Krook, On the solution of equations of transfer, *Astrophys. J.*, vol. 122, pp. 488, 1955.

[3] E.W. Larsen, G. Thömmes, A. Klar, M. Seaïd and T. Götz, Simplified P_N approximations to the equations of radiative heat transfer and applications, *J. Comput. Phys.*, vol. 183, pp. 652 – 675, 2002.

[4] B. Dubroca and J-L. Feugas, Étude théorique et numérique d'une hiérarchie de modèles aux moments pour le transfert radiatif, *C.R.Acad.Sci. Paris*, vol. 329, pp. 915 – 920, 1999.

[5] E. Olbrant, C.D. Hauck and M. Frank, A realizability – preserving discontinuous Galerkin method for the M1 model of radiative transfer, *J. Comput. Phys.*, vol. 231, pp. 5612 – 5639, 2012.

[6] P.J. Coelho, Advances in the discrete ordinates and finite volume methods for the solution of radiative heat transfer problems in participating media, *J. Quant. Spectrosc. Radiat. Transf.*, vol. 145, pp. 121 – 146, 2014.

[7] R.O. Castro and J.P. Trelles, Spatial and angular finite element method for radiative transfer in participating media, *J. Quant. Spectrosc. Radiat. Transf.*, vol. 157, pp. 81 – 105, 2015.

[8] M.A. Badri, P. Jolivet, B. Rousseau and Y. Favennec, High performance computation of radiative transfer equation using the finite element method, *J. Comput. Phys.*, vol. 360, pp. 74 – 92, 2018.

[9] J.R. Howell, The Monte Carlo method in radiative heat transfer, *J. Heat Transf.*, vol. 120, pp. 547 – 560, 1998.

[10] M.K. Banda, A. Klar and M. Seaïd, A lattice – Boltzmann relaxation scheme for coupled convection – radiation systems, *J. Comput. Phys.*, vol. 226, pp. 1408 – 1431, 2007.

[11] M. Frank, Approximate models for radiative transfer, Bulletin of the Institute of Mathematics Academia Sinica, vol. 2, pp. 409 – 432, 2007.

[12] M.A. Hossain and H.S. Takhar, Radiation effect on mixed convection along a vertical plate with uniform surface temperature, *Heat Mass Transf.*, vol. 31, pp. 243 – 248, 1996.

[13] A.D. Andrienko, S.T. Surzhikov and J.S. Shang, Spherical harmonics method applied to the multi-dimensional radiation transfer, *Comput. Phys. Commun*., vol. 184, pp. 2287 – 2298, 2013.

[14] C. Zhang, L. Zheng, X. Zhang and G. Chen, MHD flow and radiation heat transfer of nanofluids in porous media with variable surface heat flux and chemical reaction, *Appl. Math. Model*., vol. 39, pp. 165 – 181, 2015.

[15] S.T. Surzhikov, Radiation aerothermodynamics of the Stardust space vehicle, *J. Appl. Math. Mech*., vol. 80, pp. 44 – 56, 2016.

[16] M. Sheikholeslami and S.A. Shehzad, Thermal radiation of ferrofluid in existence of Lorentz forces considering variable viscosity, *Int. J. Heat Mass Transf.*, vol. 109, pp. 82 – 92, 2017.

[17] M. Waqas, M. Khan Ijaz, T. Hayat and A. Alsaedi, Numerical simulation for magneto Carreau nanofluid model with thermal radiation: A revised mode, *Comput. Methods Appl. Mech. Engrg*., vol. 324, pp. 640 – 653, 2017.

[18] M. Imtiaz, T. Hayat, S. Asad and A. Alsaedi, Flow due to a convectively heated cylinder with nonlinear thermal radiation, *Neural Comput. & Applic*., vol. 30, pp. 1095 – 1101, 2018.

[19] M. Irfan, M. Khan and W.A. Khan, Impact of non-uniform heat sink/source and convective condition in radiative heat transfer to Oldroyd – B nanofluid: A revised proposed relation, *Physics Letters A*, vol. 383, pp. 376 – 382, 2019.

[20] N.C. Roy and R.S.R. Gorla, Effects of radiation and magnetic field on mixed convection flow of non-Newtonian power-law fluids across a cylinder in the presence of chemical reaction, *Heat Mass Transf.*, vol. 55, pp. 341 – 351, 2019.

[21] M.F. Nia and S.A.G. Nassab, Conjugate problem of combined radiation and laminar forced convection separated flow, *AUT J. Model. Simul*., vol. 49, pp. 123 – 130, 2017.

[22] M.F. Nia and S.A.G. Nassab, Conjugate heat transfer study of combined radiation and forced convection turbulent separated flow, *Int. J. Nonlinear Sci. Num. Simul*., vol. 18, pp. 29 – 39, 2017.

[23] P. Wesseling, *Principles of Computational Fluid Dynamics*, Springer, Berlin, 2001.

 doi:10.20944/preprints202104.0249.v1

[24] Gh. Juncu and R. Mihail, Numerical solution of the steady incompressible Navier-Stokes equations for the flow past a sphere by a multigrid defect correction technique, *Int. J. Num. Meth. Fluids*, vol. 11, pp. 379 – 395, 1990.

[25] Gh. Juncu, Unsteady conjugate heat / mass transfer from a circular cylinder in laminar crossflow at low Reynolds numbers, *Int. J. Heat Mass Transf*. vol. 47, pp. 2469-2480, 2004.

[26] F. Pigeonneau, M. Perrodin and E. Climent, Mass-transfer enhancement by a reversible chemical reaction across the interface of a bubble rising under Stokes flow, *A.I.Ch.E. J*., vol. 60, pp. 3376 – 3388, 2014.

[27] A. Klar, J. Lang and M. Seaid, Adaptive solutions of SP_N – approximations to radiative heat transfer in glass, *Int. J. Therm. Sci*., vol. 44, pp. 1013 – 1023, 2005.

Preprints (www.preprints.org) | NOT PEER-REVIEWED | Posted: 8 April 2021 doi:10.20944/preprints202104.0249.v1

Figures Caption

Figure 1. Schematic of the problem.

Figure 2. The influence of the free stream boundary condition on the solution of the P_1 model for Re = 30, Pr = 1, r_0 = 0.5, $\mathcal{K} = 0.01$, $\mathfrak{B} = 0.9$ and $\mathcal{E} = 0.269$ (a = 0.1 m, k_a = 1 m^{-1}, β = 3 m^{-1} and ε = 0.7); (a) η_s; (b) η_N.

Figure 3. The influence of the radiation - conduction parameters $Rd_{0(1)}$ on the surface ratio for Re = 30, Pr = 1, r_0 = 0.5, $\mathcal{K} = 0.01$, $\mathfrak{B} = 0.9$ (3) and $\mathcal{E} = 0.269$ (a = 0.1 m, k_a = 1 m^{-1} , β = 3 (10) m^{-1} and ε = 0.7); (a) Φ = 1; (b) Φ = 10.

Figure 4. The influence of the conduction – radiation parameter $Rd_{0(1)}$ on the flux ratio for Re = 30, Pr = 1, r_0 = 0.5, $\mathcal{K} = 0.01$, $\mathfrak{B} = 0.9$ (3) and $\mathcal{E} = 0.269$ (a = 0.1 m, k_a = 1 m^{-1}, β = 3 (10) m^{-1} and ε = 0.7); (a) Φ = 1; (b) Φ = 10.

Figure 5. The influence of the convection rate on the surface ratio and cylinder surface dimensionless temperature for Re = 30, r_0 = 0.5, Φ =1, $\mathcal{K} = 0.01$, $\mathfrak{B} = 0.9$ and $\mathcal{E} = 0.269$ (a = 0.1 m, k_a = 1 m^{-1}, β = 3 m^{-1} and ε = 0.7); (a) η_s; (b) $\bar{Z}_{c,s}$.

Figure 6. The influence of the convection rate on the flux ratio and average Nu number for Re = 30, r_0 = 0.5, Φ =1, $\mathcal{K} = 0.01$, $\mathfrak{B} = 0.9$ and $\mathcal{E} = 0.269$ (a = 0.1 m, k_a = 1 m^{-1}, β = 3 m^{-1} and ε = 0.7); (a) η_N; (b) Nu.

Figure 7. The influence of the wire dimensionless radius r_0 on the cylinder surface dimensionless temperature and the average Nu number for P_1 model at Re = 30, Pr = 5, Φ =100, $\mathcal{K} = 0.01$, $\mathfrak{B} = 0.9$ and $\mathcal{E} = 0.269$ (a = 0.1 m, k_a = 1 m^{-1}, β = 3 m^{-1} and ε = 0.7); (a) $\bar{Z}_{c,s}$; (b) Nu.

Preprints (www.preprints.org) | NOT PEER-REVIEWED | Posted: 8 April 2021 doi:10.20944/preprints202104.0249.v1

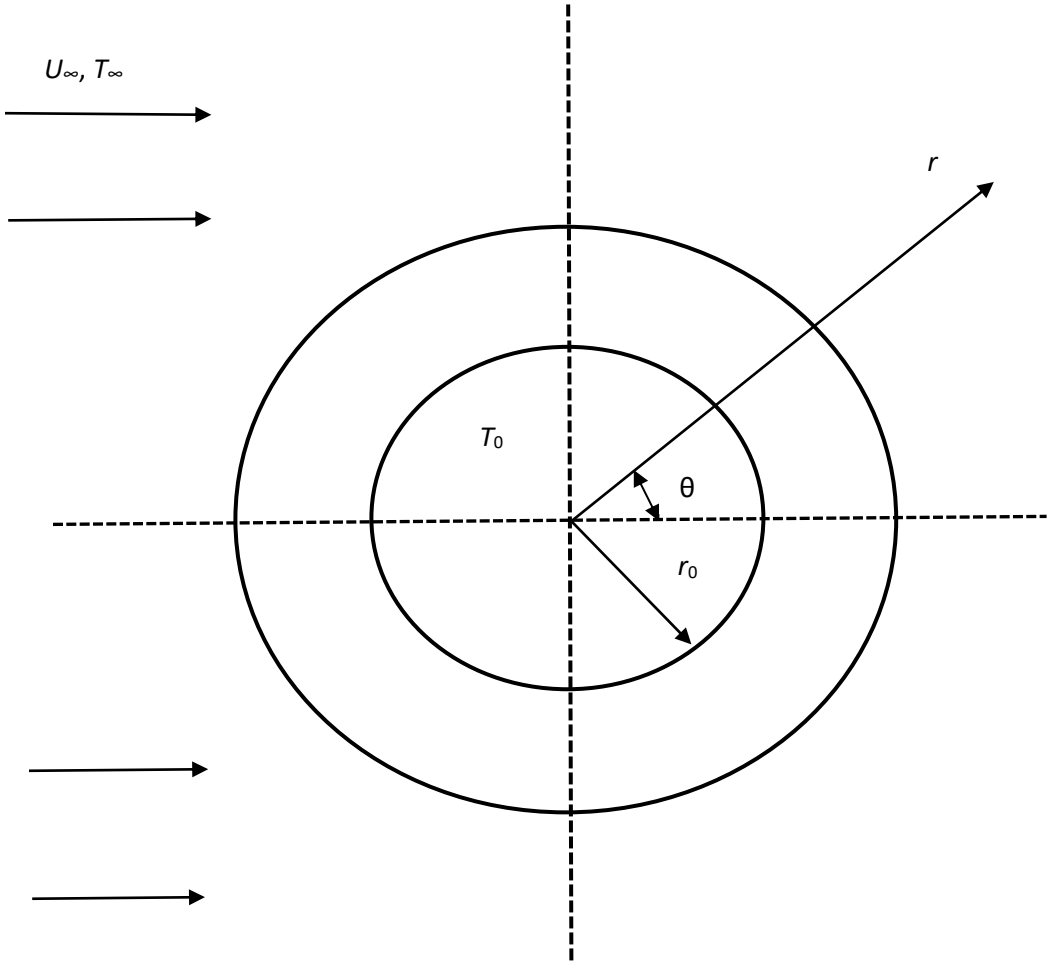

Figure 1.

Preprints (www.preprints.org) | NOT PEER-REVIEWED | Posted: 8 April 2021 doi:10.20944/preprints202104.0249.v1

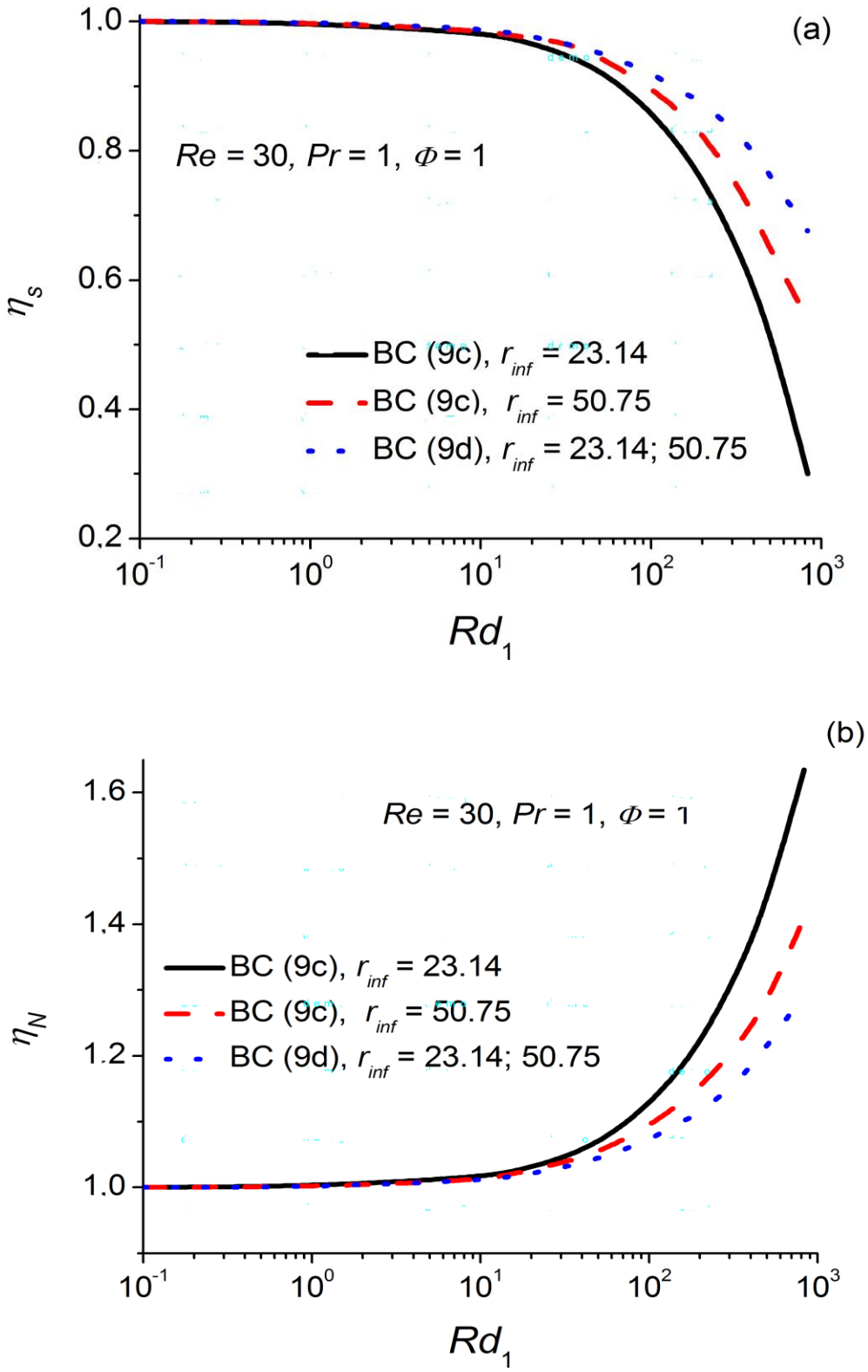

Figure 2.

Preprints (www.preprints.org) | NOT PEER-REVIEWED | Posted: 8 April 2021 doi:10.20944/preprints202104.0249.v1

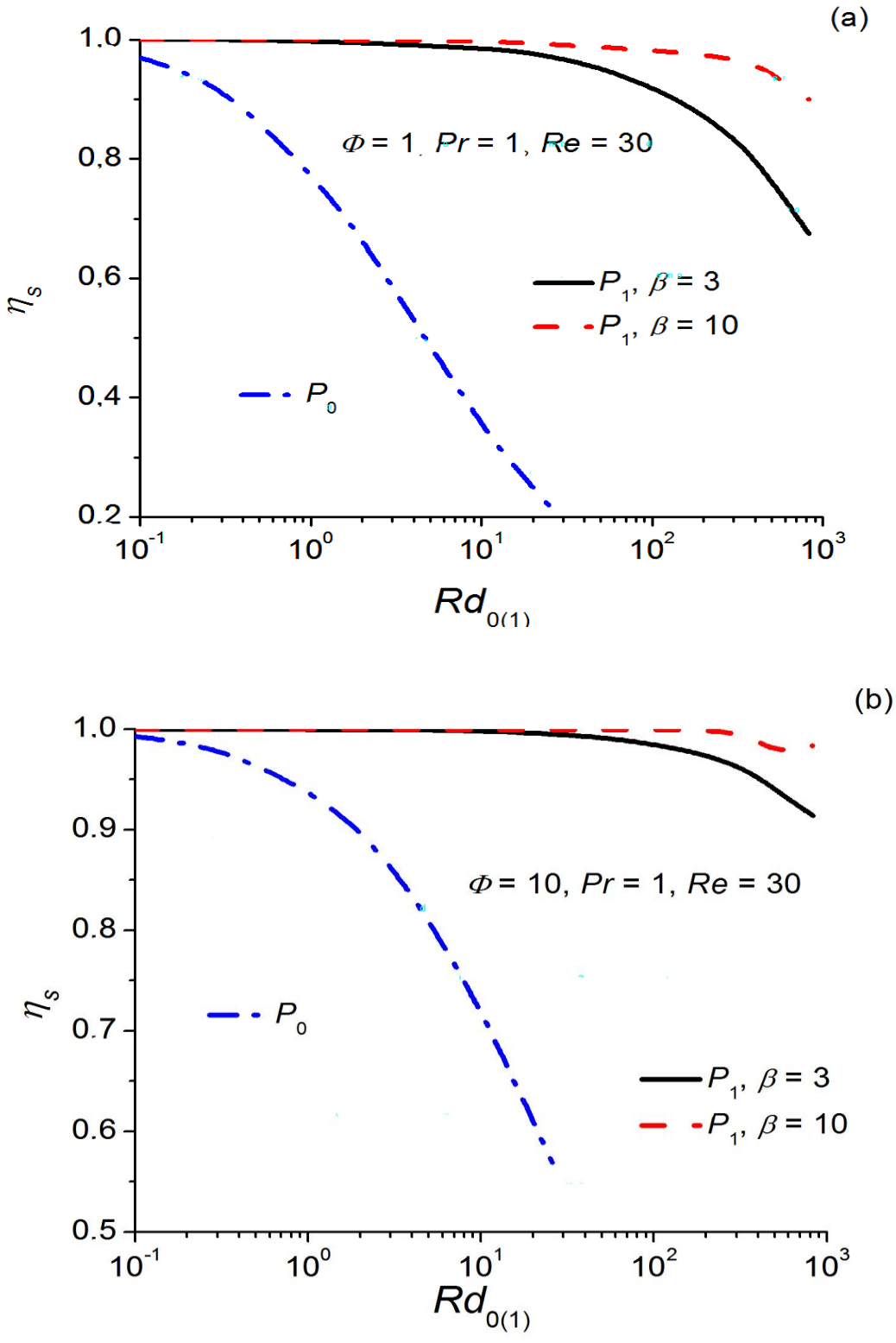

Figure 3.

Preprints (www.preprints.org) | NOT PEER-REVIEWED | Posted: 8 April 2021 doi:10.20944/preprints202104.0249.v1

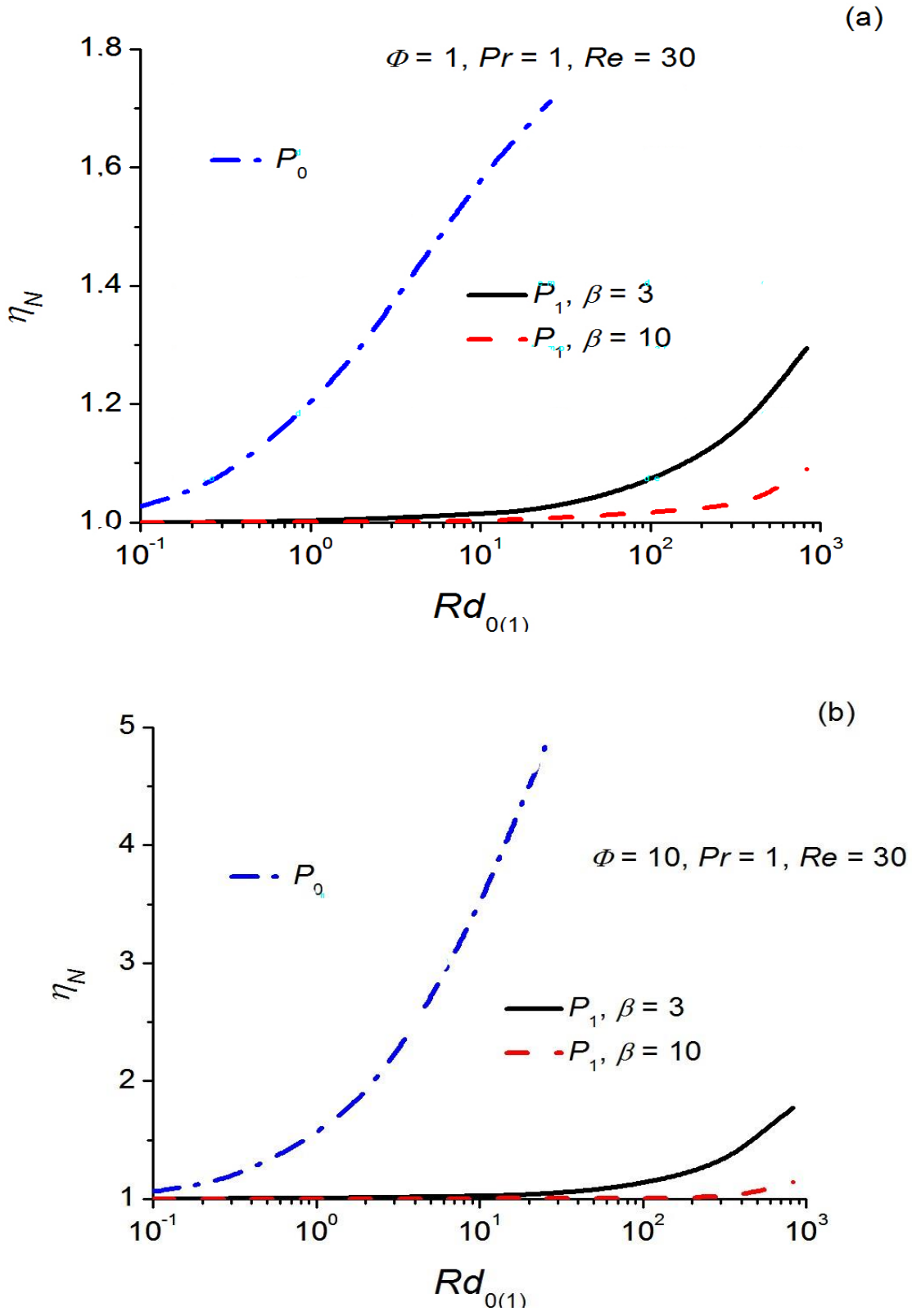

Figure 4.

Preprints (www.preprints.org) | NOT PEER-REVIEWED | Posted: 8 April 2021 doi:10.20944/preprints202104.0249.v1

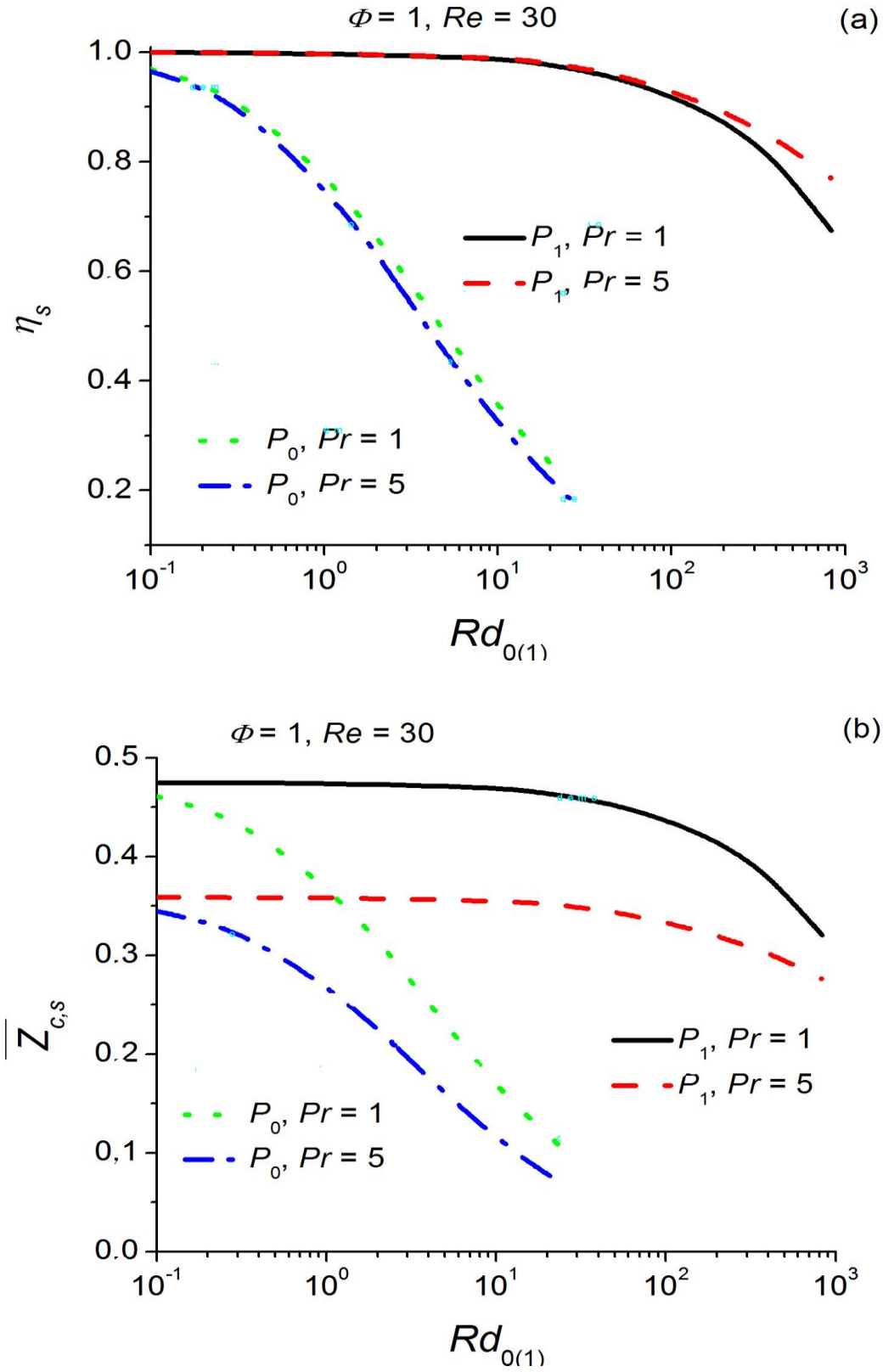

Figure 5.

Preprints (www.preprints.org) | NOT PEER-REVIEWED | Posted: 8 April 2021 doi:10.20944/preprints202104.0249.v1

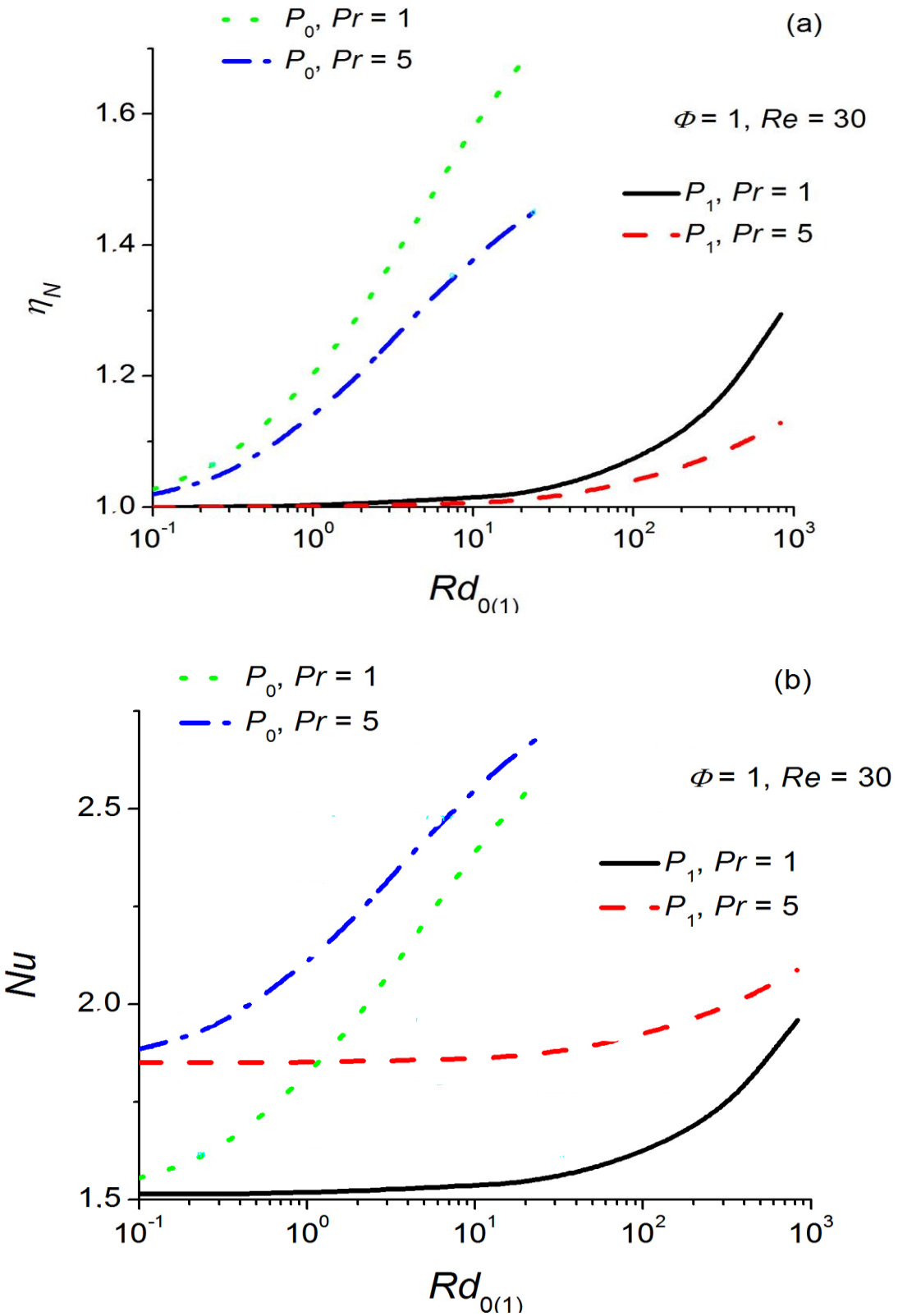

Figure 6.

Preprints (www.preprints.org) | NOT PEER-REVIEWED | Posted: 8 April 2021 doi:10.20944/preprints202104.0249.v1

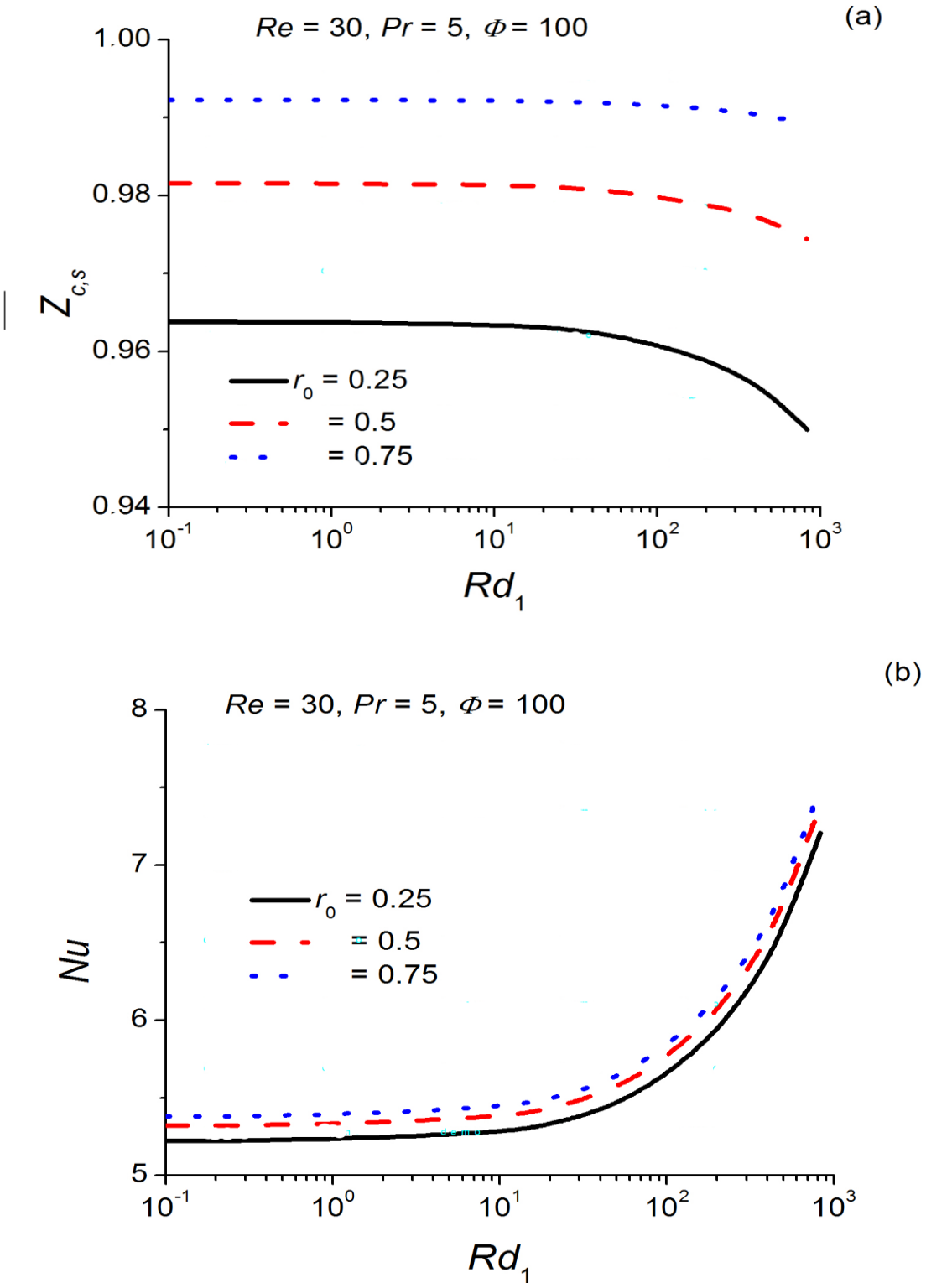

Figure 7.